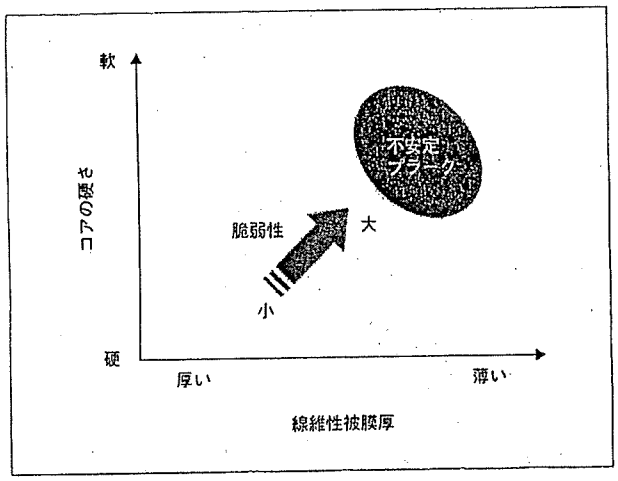


図1　不安定プラークとなる条件

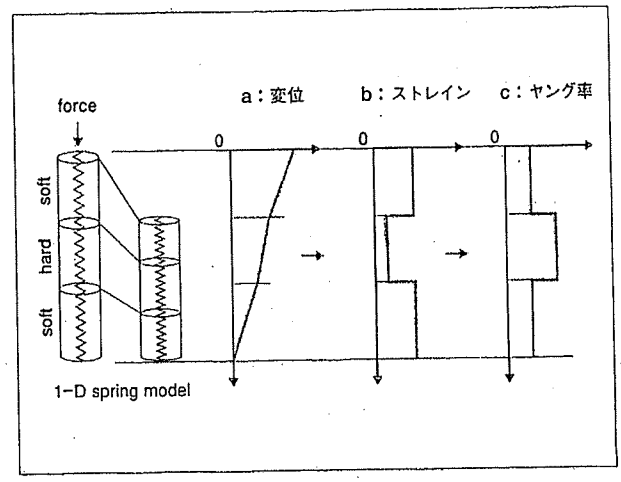


図2　組織変形に対するバネモデル

線維性被膜に覆われている状態であり，線維性被膜が十分に厚い場合は，破綻の可能性は低く安定である。このことから，不安定さの評価には，図1に示すように脂質コアの存在と，線維性被膜の薄さの双方を把握する必要がある。

脂質コアの存在診断は，いわゆる組織性状診断の1つである。IVUSでは，脂質成分は線維成分や石灰化に比べて画像輝度の低い（echolucent）部分として描出されることを利用したり，さらにエコー強度を積分したIB（integrated backscatter）を用いて，より定量化を試みている例もある。しかし，通常のIVUSで得られるBモード像はコントラストが十分でないことや，エコー強度自体は散乱（反射）特性を反映したものであり，脂質や線維成分といった組成との直接的な関連づけが明確でないなど課題が残されている。これに対して，組織の硬さ（弾性）を基に鑑別しようとするIVUS elastographyの研究がなされている[3-5]。これは，癌などで硬化した病変部の早期検出や進展範囲の同定を目的として開発された組織弾性イメージング法を応用したものである[2-6]。

すなわち，触診のように体表からわずかに圧迫した際の組織の変形を考えると，組織の局所的な変位の大部分はビームに平行な方向であるので，図2のようなバネを繋げたモデルで表すことができる。ここで，組織の変形前後の画像を比較することにより，各点の変位量を求めることができる。この変位は，超音波プローブに対しての移動量のため，臓器全体の動きを含んでいる。これは，図2でいえばバネの並行移動した分も含んでいることになるので，バネの両端に相当する2点間の変位量の差をとることにより，収縮量が求まる。これを2点間の距離で割ることで，そのバネの変形率が求まる。この変形率を，ひずみとよぶ。このひずみはバネの強さを表す指標で，ひずみが大きいものは，同じ力で変形しやすい，つまり軟らかいバネであり，小さいものは変形しにくい硬いバネということになる。実際にはバネの強さは連続的に変わると考えると，図2のように変位を空間微分することでひずみ分布を得る。組織変形もこれと同じ考えで，ひずみの大小を，組織の硬さに置き換えて捉えている。一方で，同じバネでも加える力が大きいと，ひずみも大きくなるので，ひずみそのものは，硬さの相対的な指標である。そのため，ひずみと同時に，圧迫の強さ（応力）を求めておくことで，図2cにあるようにその組織に固有な弾性特性である弾性係数（ヤング率）を得る試みもある。しかし，一般に体内における応力分布を求めるのは難しく，いくつかの仮定の下に複雑な逆問題を解く必要がある。

触診に代わるものとして，筆者らが開発した超音波組織弾性イメージング装置は，現時点ではひずみ分布像を実時間で得るものであるが，癌腫瘍のように周囲組織に比べ硬くなる病変の検出には効果的で，乳がん腫瘍の診断装置として実用化している[7]。

IVUS elastographyは，乳腺などで手で圧迫する代わりに拍動による血管組織の変形を利用している。循環器領域では，心筋ストレイン法のように，ひずみをストレインとよぶことが多いようであるが，手による圧迫か，拍動による血圧変化であるかの違いはあるが，基本的には同じで，図3に示すように拍動による血管径が変化する過程で，時刻tと，t＋Δtでの2つのフレームを取り上げ，それらのrfの超音波エコー信号を比較することで，血管壁の各点（r，θ）の時刻tにおける変位ベクトル（δr，δθ）を計測する。ここで，δr(r，θ，t)，δθ(r，θ，t)は，それぞれ半径方向，円周方向の変位を示す。

これまで，この局所変位を求める信号処理法としては，空間相関法やドプラ法（自己相関法）を応用した手法が提案されてきた。空間相関法は比較的大きな変位量を検出できるが，演算時間が多い点や誤ピークが多数出現する点で問題があり，一方，ドプラ法は高速に精度よく変位推定を行えるが，エイリアシングにより検出できる変位量が波長により制限を受ける点で問題があった。

これに対して，筆者らは，空間相関法とドプラ法の利点を融合し，実際の臨床計測でみられるような，波長以上の比較的大きな変位に対しても高速かつ高精度に，安定した計測を可能とするCA法（複合自己相関法）を開発した[6,7]。

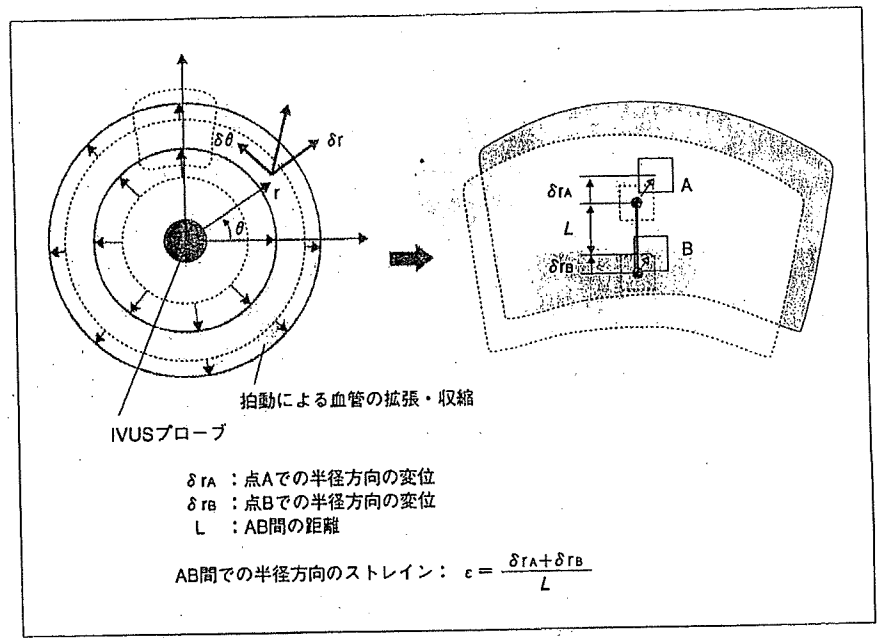


図3 IVUS elastographyの原理

ストレインは，図3に示すように2点間の変位の差分を，2点間の距離で割って求めるため，血管全体の動きは相殺されるが，短軸の場合のストレインは，血管の伸縮の方向に従って，半径方向と円周方向に分けられる。プラークがなく血管を一様な円管とみなせる場合を除いて，組織の伸縮を正確に把握するには，半径方向と円周方向のストレインを得るのが理想的である。しかし，半径方向がビーム軸方向となるIVUSの原理上，方位方向である円周方向の変位δθの計測精度は，半径方向δrに比べ極端に低下するため，雑音に弱いストレインの算出には適さない。このため，δrの計測の際にδθも得られるが，ストレインの算出は，通常，次式により半径方向のみを求めている。

$$\varepsilon_r(r,\theta,t)=\frac{\partial \delta_r(r,\theta,t)}{\partial r} \quad \cdots①$$

このストレインは，血管壁内の応力分布に依存するが，その近傍での応力の変化が急峻でないとすれば，血管断面のストレイン像は，各時刻での硬さの分布を相対的に示しているといえる。一方で，拍動の時相によって変化するので，これを瞬時ストレイン像とよぶことにする。この瞬時ストレインにより臨床上評価する場合は，どの時相で

みるかで異なり，血圧変化がなくなる最大および最小血圧近傍では部位によらず0に接近しノイズレベル以下になってしまう。そこで，われわれは拍動による時相の影響を受けずに冠動脈壁やプラークの弾性を表す特徴量として，1心拍内における歪み値変動のパワーを算出しその分布像を得るストレインパワー像を提案した[8]。

これは血管壁内の各点(r，θ)での瞬時ストレインを追跡して時系列信号εr(r，θ，t)を求めると，例えば脂質コアのような軟らかい部位では，瞬時ストレインの1心拍内の変動振幅は，線維性などのより硬い部分よりも大きくなる。変動の主要な部分は心拍周波数成分であるため，瞬時周波数の変動のスペクトル$p(r, \theta, f)$を求め，心拍周波数近傍のパワーを式②のように局所ごとに算出することによって，心拍に影響されないストレインパワー値$P(r, \theta)$を求めることができる。

$$P(r,\theta) = \int_{fc-\Delta f}^{fc+\Delta f} p(r,\theta;f)\,df \cdots ②$$

ここで，fcは心拍周波数，Δfはfc周りのパワー計算幅である。

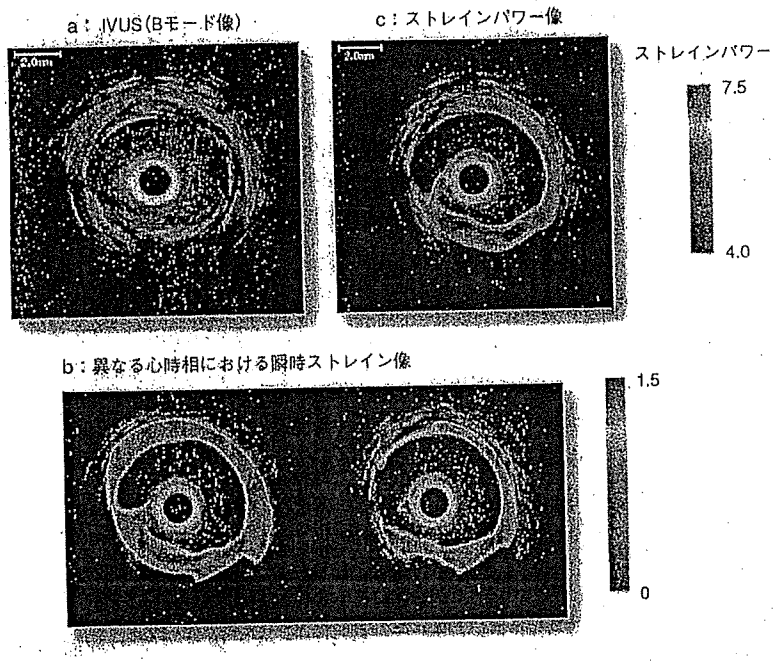


図4　冠動脈のIVUSによるBモード，ストレインパワー像
複合したプラークを有する症例。

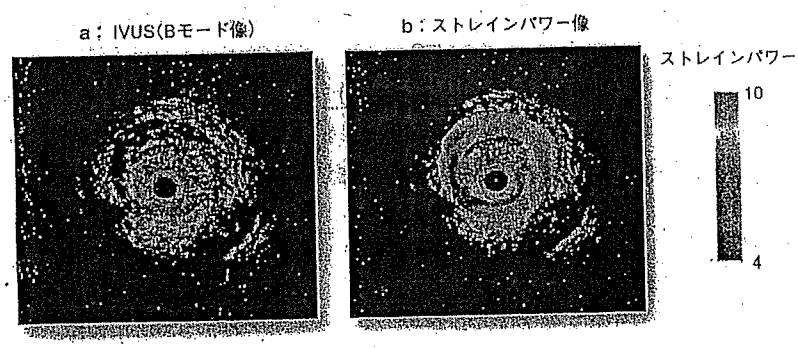


図5　冠動脈のIVUSによるBモードおよびストレインパワー像
脂質性の不安定プラークを有する症例。

## IVUS elastographyによる冠動脈プラークの評価

臨床データを解析できる装置として，(株)テルモ製の中心周波数40MHzのIVUSプローブを用い，rfでの超音波エコー信号を計測するため，240MHz，12bitでA/D変換し，連続して600フレーム(約20秒)のデータを取得できるシステムを開発した。臨床データの取得は，通常の冠動脈インターベンション中に行われるが，実施医療機関の倫理委員会での承認，および患者への十分なインフォームドコンセントの下に実施された。

図4aは線維化および石灰化したプ

ラークを含む症例の冠動脈のIVUS（Bモード像）である。コントラストは十分ではないが，動画として観察すると，10時方向から5時方向にわたって軟らかい細胞成分を含む線維化，5時方向から7時方向にわたって硬い石灰化を含む線維化を生じている様子が推測できる。図4bは2つの異なる心時相における瞬時ストレインを示し，右側は左に比べ血圧が急速に変化する時相に相当する。ストレインの高値を赤，低値を青で表示し，Bモードに重ねて表示している。右側では石灰化の部分が青く，硬い組織であることが描出されているが，左側では血圧差が小さいため不鮮明である。また，9時方向が不鮮明になっているのは，ガイドワイヤによる陰の影響である。ストレインパワー像を求めたものを図4cに示す。パワーの高値を赤に，低値を青でBモード像に重ねて表示してある。細胞成分および石灰化を含む2つの線維化領域が明瞭なコントラストで識別できることがわかる。

次に，図5は，10時から3時付近にかけて肥厚した脂質性不安定プラークを有する症例の結果を示す。同じく，図5aは通常のBモード像，図5bはそれにストレインパワーをカラー表示したものである。脂質性プラークの部位に対応して赤く可動性の大きい領域として描出され，歪みパワー像などの組織弾性イメージングが不安定プラークの検出手段として有望であることが示されている。

前述より，ストレインパワー像により，1心拍の平均的な特性として心時相によらず，異なるプラーク組成が識別される可能性が示唆されたといえる。一方で，*in vivo*での計測であり，今後は剖検例など*in vitro*計測と比較して検証を重ねる必要がある。

## 結論

硬さに基づくプラークの組織性状の違いを可視化するIVUS elastographyの原理と，不安定プラーク性状評価への応用について示してきたが，変形性という間接であるが硬さの指標を画像化することで，脂質性プラークなどの不安定性を評価する手段となりうることが示された。一方で，易破綻性の指標としては，硬さそのものより，プラークでの角の部位など，変形性の高い部位であり，その意味ではより直接的である可能性も出てくる。また，不安定プラークにおいて特に破綻しやすい部位の検出を可能とするためには，一層の高分解能化と血圧値を同時計測することによる定量化，線維性被膜や脂質コアの力学的特性と実際の不安定性との関連の把握に努める必要があろう。

## 文献


1) 上田真喜子，齋藤 顕：急性冠症候群の病態生理から見た治療戦略，Medical Tribune 32: 26, 1999.
2) de Korte CL, Pasterkamp G, van der Steen AF, Woutman HA, Bom N: Characterization of plaque components with intravascular ultrasound elastography in human femoral and coronary arteries in vitro. Circulation 102: 617-623, 2000.
3) Shapo BM, Crowe JR, Skovoroda AR, et al: Displacement and Strain Imaging of Coronary Arteries with Intraluminal Ultrasound, IEEE Trans Ultrason Ferroelect Freq Contr 43: 234-246, 1996.
4) Shiina T, Nitta N, Yamagishi M: Coronary Arteries Characterization Based on Tissue Elasticity Imaging-in-vivo Assessment-. Proc of 2002 IEEE Ultrasonics Symp 1811-1814, 2002.
5) 新田尚隆，遠藤浩幸，椎名 毅，山岸正和：血管内エコー法を用いた冠動脈弾性イメージング．電子情報通信学会論文誌 J87-D-II: 78-87, 2004.
6) 椎名 毅，新田尚隆，植野 映，Bamber JC：複合自己相関法による実時間 Tissue Elasticity Imaging．日本超音波医学会，26: 57-66, 1999.
7) Yamakawa M, Shiina T: Strain Estimation Using the Extended Combined Autocorrelation Method. Jpn J Appl Phys 40: 3872-3876, 2001.
8) Shiina T, Nitta N, Yamagishi M: A New Method for Deter mining Vulnerable Atherosclerotic Plaque by Intravascular Ultrasound Elasticity Imaging, Imaging Vulnerable Atheroscle rotic Plaque-The Evolving of New Imaging Technique-, Abstract of the 68th annual scientific meeting of Japanese Circulation Society. SY3-5, 2004.

第14回コンピュータ外科学会講演論文集
CAS/CADM合同シンポジウム　2005.11.20

# 05(JS)-2　画像診断の進歩：血管超音波 elastograpy

○椎名　毅[1]，新田尚隆[2]，山岸正和[3]
1 筑波大学 大学院システム情報工学研究科
2 産業技術総合研究所 人間福祉医工学研究部門
3 国立循環器病センター 心臓血管内科部門

## Progress of Medical Imaging - Intravascular Ultrasound Elastography-

T.Shiina[1], N.Nitta[2], M.Yamagishi[3]
*1 Graduate School of Systems and Information Engineering, University of Tsukuba, Tsukuba, Japan*
*2 NationalInstitute of Advanced Industrial Science and Technology, Tsukuba, Japan*
*3 National Cardiovascular Center, Osaka, Japan*

**Abstract:** Most cases of acute coronary syndrome occur suddenly, even when the stenos is not so serious, then plaque rupture is regarded as one of main causes. To prevent plaque rupture and guide a pharmacological treatment, it is important to image the weak (fragile) part of atheroscleotic plaque and to determine between high-risk and low-risk plaques. Intravascular Ultrasound Elasticity Imaging has the potential to differentiate between plaques types. Preliminary experiments revealed that it is feasible to discriminate between fatty, fatty fibrous, calcified material by this technique. Plaque rapture is related to a fragility of the thin fibrous cap over lipid core. Its fragile part of vulnerable plaque is expected to be imaged as more deformable area with high strain
**Keywords :** Intravascular ultrasound, atheroscleotic plaque, tissue elasticity, Vulnerable Coronary Plaque

## 1. はじめに

虚血性心疾患は、以前は冠動脈内に生じたプラークによる内腔の狭窄が主因と考えられ、経皮的冠動脈形成術（PTCA）などの冠動脈インターベンションが成果を挙げてきた。しかしその一方で高度狭窄でなくとも急性心疾患症が発生しうることから、近年の研究成果により、不安定狭心症や急性心筋梗塞のほとんどは、プラーク破綻（plaque rapture）を引き金とした血栓形成により、冠動脈内腔が狭窄及び閉塞されて生じる、いわゆる急性冠症候群（ACS）であることが明らかとなってきた。特に、脂質が薄い線維被膜に覆われたプラークは破綻し易い不安定プラークとなると考えられている。このため急性冠症候群の予防には、安定度を決定している脂質，線維化，石灰化などの異なるプラーク組成を正確に識別し，プラークの安定度に関して適切な診断を下す必要がある。

現在までに、心臓カテーテルでの低侵襲的な方法として、冠動脈内視鏡、OCT，血管内エコー（IVUS）など様々な手法で冠動脈プラークの性状を診断する技術が開発されているが、特に近年では、組織の硬さという力学的特性から、より直接的に破綻しやすい不安定プラークを検出する方法として、血管内超音波 elastography（ IVUS elastography）の研究が注目されている。ここでは、血管内超音波エラストグラフィの原理と、臨床計測の実例を通して、プラーク性状評価への応用の現状と展望について概説してみたい。

## 2．血管超音波elasographyの原理

不安定プラークは、図１に示したように脂質コアが薄い繊維性被膜に覆われている状態であり、繊維性被膜が十分に厚い場合は、破綻の可能性は低く安定である。このことから、不安定さの評価には、脂質コアの存在と、繊維性被膜の薄さの双方を把握する必要がある。血管内超音波 elastography は、拍動による血圧変動により血管組織が変形する割合である歪みを画像化している。これは、一定の応力では、硬い（ヤング率が

大きい）ものほど変形しにくい、すなわち歪み小さいことを利用している。したがって脂質成分は、繊維成分、石灰化成分などに比べると最も柔らかく、歪みが大きくなりやすい。

一方、繊維性被膜の厚みの評価については、冠動脈や頚動脈ともに250μm程度以下になると不安定になるとの報告がなされている。IVUSに用いる約40MHzの超音波では空間分解能的に難しいが、脂質コアかつ繊維性被膜が薄い場合には、歪みが増大するため、やはり歪みを指標にして不安定性を評価可能ということになる。また、歪みの大きな部位は、それだけ変形が大きく破綻が生じやすい部位とも言える。実際、破綻部位はプラークの角の部分で多く発生することが知られているが、歪みは力学的な脆弱性を表すので、将来的には、より具体的に破綻危険度の高い部位を可視化する手段と可能性も秘めていると言えよう。

## 3．冠動脈プラークの評価

通常の冠動脈インターベンション中に、IVUSで得られるエコー信号を利用した。中心周波数 40 MHzのIVUSプローブを用いて、240MHz、12bitでA/D変換したものを連続して600フレーム（約20秒）のデータを取得し、歪み分布を得た。一方、歪みは拍動に伴う血圧変化による変動するため、1心拍内における歪み値変動のパワーであるストレインパワー像を求めた。これにより、1心拍での平均的な変形率が安定に表示される。

図2は、10時から3時付近にかけて肥厚した脂質性不安定プラークを有する症例の結果を示す。 (a)は通常のBモード像、(b)はそれにストレインパワーをカラー表示したものである。脂質性プラークの部位は、赤く可動性の大きい領域として描出されており、血管内 elastography が不安定プラークを検出手段として有望であることが示されている。

## 4．結論

硬さに基づくプラークの組織性状の違いを可視化する血管内超音波 elstographyについて概説し、臨床データの解析により歪みという間接であるが硬さの指標を画像化することで、脂質性プラークなどの不安定性を評価する手段となりうることが示された。また、易破綻性の指標としては、硬さそのものより、プラークでの角の部位など、変形性の高い部位であり、その意味ではより直接的である可能性も出てくる。

今後、検討すべきなものとしては易破綻性と組織弾性および病理組織学的な対応づけが重要であり、*in vitro*計測と比較して検証を重ねる必要がある

## 参考文献


[1] C.L. de Korte, et al: "Characterization of Plaque Components With Intravascular Ultrasound Elastography in Human Femoral and Coronary Arteries In Vitro". Circulation, pp. 618-623, 2000.

[2] T.Shiina, et al.: "Assessment of Vulnerable Coronary Plaque by Intravascular Elasticity Imaging,"Proc. of IEEE International Symposium, pp.364-367, 2004.


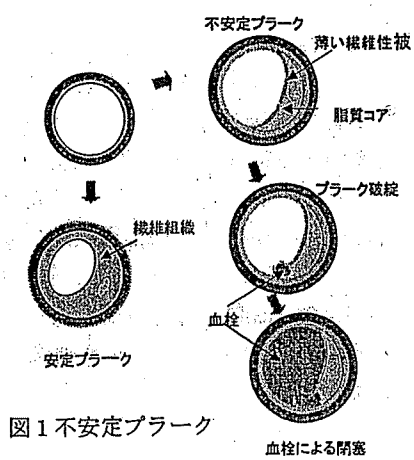


図1 不安定プラーク

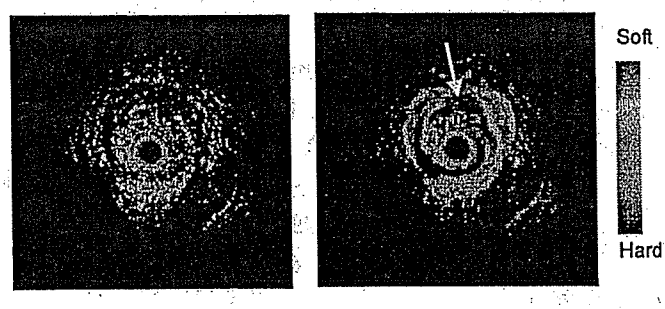


(a) IVUS(B-mode) image (b)Strain power image

図2 冠動脈のIVUSによるBモードおよびストレインパワー像：脂質性の不安定プラークを有する症例

*Images in Cardiovascular Medicine*

# A Potential Complication of Directional Coronary Atherectomy

## for In-Stent Restenosis

**Yuxin Li, MD**
**Junko Honye, MD**
**Tadateru Takayama, MD**
**Shin-Ichiro Yokoyama, MD**
**Satoshi Saito, MD**

We report the case of a patient who underwent directional coronary atherectomy (DCA) for in-stent restenosis of the left anterior descending coronary artery (LAD). After right femoral arterial access, a 10F guiding catheter was used to pass the in-stent restenotic lesion with a 0.014" guide wire. The DCA was performed with a 7F AtheroCath-GTO® atherectomy catheter* (Guidant Corporation; Temecula, Calif). Intravenous ultrasonography (IVUS) was used to optimize the tissue resection. Multiple circumferential cuts were made at pressures from 10 psi to 30 psi. The atherectomy procedure progressed smoothly at a pressure of 10 psi (10 times) and 20 psi (8 times). However, after the 1st cut at a pressure of 30 psi, the cutter suddenly stopped, and the cutter could not be pushed forward or pulled back. The operator then pulled back the whole DCA system into the guiding catheter. No palpable resistance was encountered upon withdrawing the atherectomy catheter; however, fluoroscopic monitoring revealed that the stent was being avulsed from the coronary artery with the atherectomy catheter. After the DCA catheter had been removed, the previously implanted Multi-Link® stent (Guidant Corp.) was found to be trapped between the cutter and the housing (Fig. 1). The stent was removed from the coronary artery. The final angiogram and IVUS revealed that no coronary perforation or other severe complications of the vessel had occurred (Fig. 2).

***Fig. 1*** *Multi-Link® stent (Guidant Corp.) that was pulled out with the whole directional coronary atherectomy catheter system. It is distorted with slight breakage. Part of the plaque and neointima were also pulled out with the stent.*

*This product was placed on the FDA recall list in June 2001 because of dislodgment of the catheter tip in a patient.

***Section Editor:*** *Raymond F. Stainback, MD, Department of Adult Cardiology, Texas Heart Institute and St. Luke's Episcopal Hospital, 6624 Fannin Street, Suite 2480, Houston, TX 77030*

***From:*** *Division of Cardiology, the Second Department of Medicine, Nihon University School of Medicine, Tokyo, Japan 173-8610*

***Address for reprints:*** *Satoshi Saito, MD, Division of Cardiology, the Second Department of Medicine, Nihon University School of Medicine, 30-1 Oyaguchi-Kami-machi, Itabashi-ku, Tokyo, Japan 173-8610*

*E-mail: Satoshis@med.nihon-u.ac.jp*

## Discussion

Since approximately 1 million coronary stents are implanted worldwide every year,[1] the management of in-stent restenosis has become a significant challenge for interventional cardiologists. Tissue proliferation is the major cause of in-stent restenosis; therefore, a debulking technique such as directional coronary atherectomy (DCA) would seem to offer a therapeutic advantage by removing the neointimal tissue. Some studies have confirmed the efficacy of DCA for the treatment of in-stent restenosis.[1-3]

The safety of DCA procedures may be dependent on the stent design and construction. Success with DCA has been reported in patients with slotted tube[4] and Palmaz-Schatz[1] stent restenosis. However, implanted stent and vessel disruption have been reported after the use of DCA for the treatment of in-stent restenosis of coil stents.[5,6] In 1 series,[7] 2 out of 50 patients had stents that were apparently deformed by the atherectomy procedure. There were also some small complications or technical difficulties such as the atherectomy devices' becoming blocked several times at higher balloon pressures.[7] In our patient, the previously implanted stent was entrapped and was pulled from the coronary artery. On the basis of our case and previous reports, cardiologists should bear in mind that it is possible for struts to block the cutter. When DCA is used for in-stent restenosis, aiming for optimal debulking may lead to this rare complication. Therefore, a conservative debulking strategy might be safer.

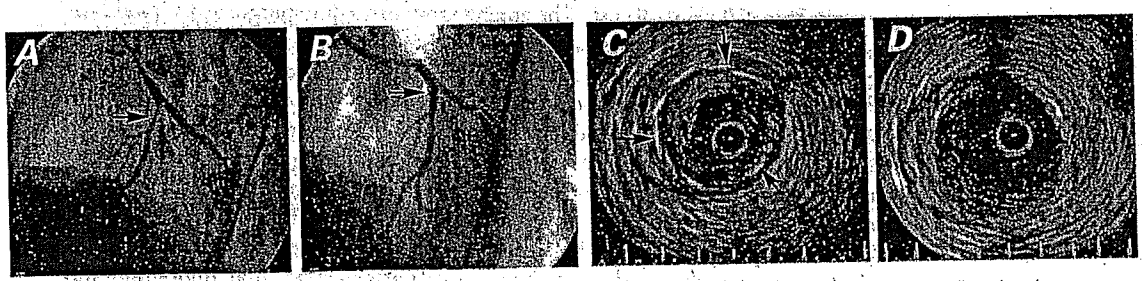


*Fig. 2* Angiograms and intravascular ultrasonographic (IVUS) images of in-stent restenosis before and after directional coronary atherectomy (DCA). **A)** Angiogram shows 90% diffuse in-stent restenosis in the left anterior descending coronary artery segment 6 (arrow). **B)** The restenosis is abolished after DCA (as shown by arrow). **C)** Before DCA, IVUS shows the stent (arrows) and severe neointimal proliferation within the stent. **D)** The enlarged lumen is shown after DCA, when the stent and neointima were pulled out.

## References


1. Mahdi NA, Pathan AZ, Harrell L, Leon MN, Lopez J, Butte A, et al. Directional coronary atherectomy for the treatment of Palmaz-Schatz in-stent restenosis. Am J Cardiol 1998;82:1345-51.
2. Mintz GS, Hoffmann R, Mehran R, Pichard AD, Kent KM, Satler LF, et al. In-stent restenosis: the Washington Hospital Center experience. Am J Cardiol 1998;81(7A):7E-13E.
3. Dauerman HL, Baim DS, Cutlip DE, Sparano AM, Gibson CM, Kuntz RE, et al. Mechanical debulking versus balloon angioplasty for the treatment of diffuse in-stent restenosis. Am J Cardiol 1998;82:277-84.
4. Palacios IF, Sanchez PL, Mahdi NA. The place of directional coronary atherectomy for the treatment of in-stent restenosis. Semin Interv Cardiol 2000;5:209-16.
5. Macander PJ, Roubin GS, Agrawal SK, Cannon AD, Dean LS, Baxley WA. Balloon angioplasty for treatment of in-stent restenosis: feasibility, safety, and efficacy. Cathet Cardiovasc Diagn 1994;32:125-31.
6. Bowerman RE, Pinkerton CA, Kirk B, Waller BE. Disruption of a coronary stent during atherectomy for restenosis. Cathet Cardiovasc Diagn 1991;24:248-51.
7. Haberbosch W, Waas W, Waldecker B, Helzmann H, Holschermann H, Rau M, Tillmanns H. Directional coronary atherectomy of in-stent restenosis: a two-center experience. J Interv Cardiol 2000;13:93-9.

ELSEVIER

International Journal of Cardiology xx (2005) xxx – xxx

International Journal of Cardiology

www.elsevier.com/locate/ijcard

Letters to the Editor

# Whole-heart coronary magnetic resonance angiography in a patient with unstable angina

Yuichi Sato *, Naoya Matsumoto, Shunichi Yoda, Satoshi Kunimoto, Yuji Kasamaki, Tadateru Takayama, Satoru Furuhashi, Motoichiro Takahashi, Takahisa Uchiyama, Satoshi Saito

*Department of Cardiology, Nihon University School of Medicine, 1-8-13 Kanda-Surugadai, Chiyoda-ku, Tokyo 101-8309, Japan*

Received 22 June 2005; accepted 25 June 2005

*Keywords:* Whole-heart coronary MR angiography; Unstable angina

## 1. Case report

A 67-year-old man was transferred to the emergency department because of anterior chest pain which persisted for 30 min. He had no significant coronary risk factors. Upon admission, there were no ST segment elevations or T wave abnormalities. Initial serum creatine kinase was 116 IU/l and troponin I was negative. Echocardiography revealed no left ventricular regional wall motion abnormality. The patient was referred to whole-heart coronary magnetic resonance angiography (MRA) with a provisional diagnosis of unstable angina. MRA was performed using a free-breathing, 3-dimensional navigator technique [1]. Volume rendering image showed stenosis in the proximal portion of the left anterior descending artery (Fig. 1A, arrow). Maximum intensity projection image demonstrated high-grade stenosis in the left anterior descending artery immediately distal to the bifurcation point (Fig. 1B, arrow). Conventional coronary angiography revealed subtotal occlusion of the left anterior descending artery (Fig. 2, arrow).

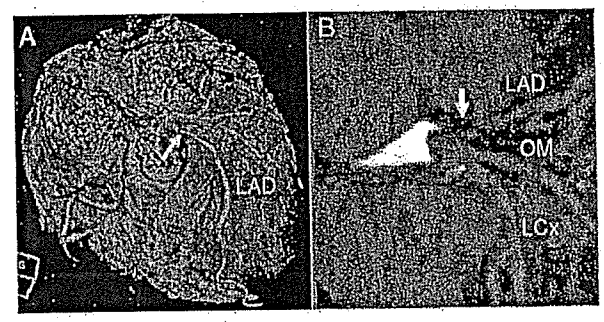


Fig. 1. LAD=left anterior descending artery, LCx=left circumflex artery, and OM=obtuse marginal artery.

## 2. Discussion

The diagnosis of acute coronary syndrome (ACS) especially non-ST-elevation myocardial infarction and unstable angina in the emergency department still remains a challenge.

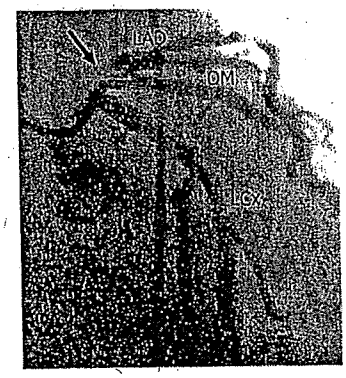


Fig. 2. LAD=left anterior descending artery, LCx=left circumflex artery, and OM=obtuse marginal artery.

* Corresponding author. Tel.: +81 3293 1711; fax: +81 3295 1859.
*E-mail address:* yuichis@med.nihon-u.ac.jp (Y. Sato).


doi:10.1016/j.ijcard.2005.06.069

Despite the initial risk assessment using ECG and cardiac enzymes, approximately 2% of patients with ACS are inappropriately discharged home from the emergency department [2]. On the other hand, aggressive, invasive procedure is not fully justified because it may expose patients with low likelihood of ACS to angiography-related complications and excessive medical expense. Whole-heart coronary MRA allows totally non-invasive assessment of coronary artery disease and has the potential to become a routine diagnostic tool in patients with suspected ACS in the emergency department.

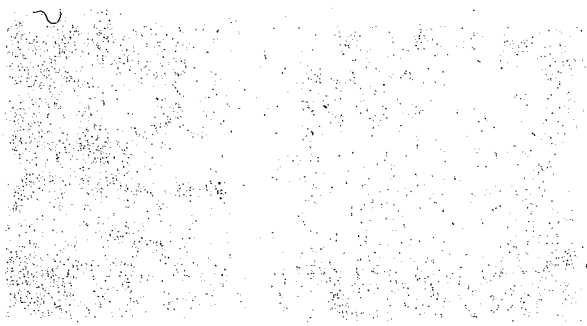

## References

[1] Weber OM, Pujadas S, Martin AJ, Higgins CB. Free-breathing, three-dimensional coronary artery magnetic resonance angiography: comparison of sequences. J Magn Reson Imaging 2004;20:395–402.

[2] Pope JH, Aufderheide TP, Ruthazer R, et al. Missed diagnosis of acute cardiac ischemia in the emergency department. N Engl J Med 2000; 342:1163–70.

Journal of the American College of Cardiology
© 2005 by the American College of Cardiology Foundation
Published by Elsevier Inc.

Vol. 45, No. 12, 2005
ISSN 0735-1097/05/$30.00
doi:10.1016/j.jacc.2004.10.080

# Detection of Lipid-Laden Atherosclerotic Plaque by Wavelet Analysis of Radiofrequency Intravascular Ultrasound Signals

## In Vitro Validation and Preliminary In Vivo Application

Akihiro Murashige, MD, Takafumi Hiro, MD, PHD, Takashi Fujii, MD, PHD, Koji Imoto, MD, Takashige Murata, MD, Yusaku Fukumoto, MD, Masunori Matsuzaki, MD, PHD

*Yamaguchi, Japan*

**OBJECTIVES** This study examined the feasibility of using a wavelet analysis of radiofrequency (RF) intravascular ultrasound (IVUS) signals in detecting lipid-laden plaque.

**BACKGROUND** Wavelet analysis is a new mathematical model for assessing local changes in a geometrical profile of time-series signals.

**METHODS** Radiofrequency IVUS signals of 85 arbitrarily selected vectors were acquired from 27 formalin-fixed noncalcified atherosclerotic plaques from human necropsy with a digitizer at 500 MHz with 8-bit resolution by use of a 40-MHz IVUS catheter. Wavelet analysis of these RF signals was performed using a Daubechies-2 wavelet to obtain a color-coded map of the correlation coefficient with the wavelet reconstructed over the x-y plane of the wavelet scale and the distance from the IVUS catheter. The plaque segment was then examined histologically after being stained with Masson's trichrome stain. This technique also was applied in vivo in 29 human coronary plaque segments. These segments were excised subsequently by directional coronary atherectomy and processed for histologic analysis.

**RESULTS** In the in vitro study, histologic examination revealed lipid-laden segments in 29 vectors. When performing a wavelet analysis with the Daubechies-2 wavelet, the color-coded mapping revealed a different pattern in lipid-laden plaques compared with other types of plaque. Using this wavelet analysis, lipid-laden plaque could be detected with a sensitivity of 83% (24 of 29) and a specificity of 82% (46 of 56). In the in vivo study, fatty plaque could be detected with a sensitivity of 81% (13 of 16) and a specificity of 85% (11 of 13) with this method.

**CONCLUSIONS** Wavelet analysis of RF IVUS signals enabled in vitro as well as in vivo detection of lipid-laden plaque. This method may be useful in assessing plaque vulnerability in patients with coronary artery disease. (J Am Coll Cardiol 2005;45:1954–60) © 2005 by the American College of Cardiology Foundation

Because lipid-rich plaques with thin fibrous caps have been shown to be vulnerable to rupture as a major cause of acute coronary events (1,2), several attempts have been made to develop an imaging modality to identify such plaques before

See page 1970

they rupture. Intravascular ultrasound (IVUS) imaging provides a detailed arterial cross section with accurate morphometric representation of atherosclerotic plaque dimensions in vitro and in vivo (3–15). However, subsequent studies have demonstrated significant limitations in tissue characterization by IVUS intensity patterns alone, especially in discriminating fibrous and fatty tissues (16–19). To overcome these limitations, many authors (19–24) have proposed methods of quantitative tissue characterization to discriminate fibrous and fatty plaque. However, none of these methods has been sufficiently well recognized as of yet for the appropriate equipment to be installed in commercially available IVUS machines.

Wavelet analysis is a new mathematical model for assessing local changes in the geometrical profile of time-series signals (25). Wavelet analysis is one of the time-frequency domain analyses of signals. This method discriminates a local unique wave pattern within a complex signal. The purpose of this study was to investigate the feasibility of using wavelet analysis of radiofrequency (RF) IVUS signals to detect lipid-laden plaque. The reliability of this method was first examined with in vitro atherosclerotic plaque segments from human necropsy. The parameters evaluated in this in vitro model were applied to an in vivo clinical setting and tested against the histology of the coronary segments excised with directional coronary atherectomy. The histology of the excised tissue was compared with the results of the wavelet analysis of RF IVUS signals.

From the Division of Cardiovascular Medicine, Department of Medical Bioregulation, Yamaguchi University Graduate School of Medicine, Yamaguchi, Japan. This work was partly supported by a grant-in-aid for scientific research of the Ministry of Education, Japan (grant No. 13670715). Health and Labour Sciences research grants: Comprehensive Research on Cardiovascular Diseases from Ministry of Health, Labour, and Welfare of Japan, and Knowledge Cluster Initiative of the Ministry of Education, Japan. This study was presented in part at the 75th scientific sessions of the American Heart Association, Chicago, Illinois, 2002. Drs. Murashige and Hiro contributed equally to this work.

Manuscript received June 13, 2004; revised manuscript received October 19, 2004, accepted October 25, 2004.

Abbreviations and Acronyms
IVUS = intravascular ultrasound
RF = radiofrequency

## METHODS

**In vitro IVUS study.** Twenty-seven formalin-fixed noncalcified atherosclerotic plaques that were obtained from human femoral and coronary arteries excised from 10 patients at necropsy were imaged using a 40-MHz Atlantis Plus IVUS catheter (CVIS/Boston Scientific, Sunnyvale, California) in saline at room temperature. Eight of these patients died of heart failure with ischemic cardiomyopathy or old myocardial infarction, and two died of noncardiac events. The imaged arteries had plaques with a thickness >0.5 mm. The lumen area of the examine vessel was 10.48 ± 5.78 $mm^2$ (range, 1.57 to 25.2 $mm^2$).

Calcified plaques were not studied in the present study because calcified tissue is identified readily by visual inspection with high sensitivity and specificity (13). The current concern for tissue characterization of plaque is how to discriminate between fibrous and fatty tissue. An acoustic reference point was determined by suturing a surgical needle into the wall of the artery perpendicular to the long axis. This technique ensured that the same cross section was imaged for all studies and that the ultrasound images corresponded exactly to the cross section chosen for histologic analysis.

The entire length of the artery was imaged initially by visual inspection using conventional IVUS video monitoring to find an optimal portion of atherosclerotic plaque that provided no significant change in tissue composition or structure within at least a 0.5-mm length of the artery. Care was taken to position the catheter centrally and coaxially. The ultrasound images were recorded on super VHS tape.

**Data acquisition.** We sampled in vitro cross-sectional images of 27 noncalcified plaques in 21 atherosclerotic formalin-fixed artery specimens (coronary: n = 9; femoral: n = 12) with a commercially available IVUS machine (ClearView Ultra System, CVIS/Boston Scientific) and a 40-MHz IVUS catheter. The RF IVUS signals of 256 radial vectors, which completely surrounded (360°) the catheter center with an equal angle span (1.4°), were obtained from these plaques using an analog-to-digital converter installed inside the IVUS machine (Fig. 1). The analog-to-digital board was specially designed and installed by the IVUS manufacturer. Each cross section comprised these 256 RF IVUS signals, which were sampled in real time at 500 MHz in 8-bit resolution with a digitizer and then stored on hard disk for further analysis. Each cross-sectional IVUS image also was recorded on videotape. On a video screen, a radial line from the catheter center was superimposed on a conventional cross-sectional IVUS image to enable recognition of the location of each vector. The vectors analyzed

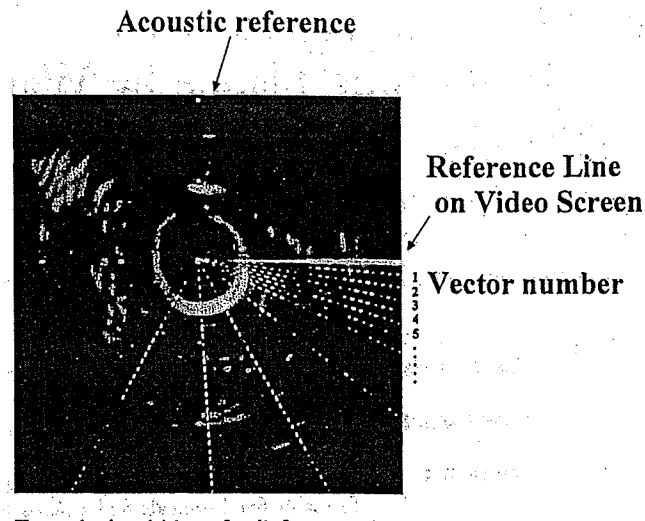


**Figure 1.** Acquisition of radiofrequency intravascular ultrasound signals. There are 256 radial vectors of radiofrequency signal sampled around the intravascular ultrasound catheter.

were first obtained from the thickest portion of the plaque imaged. We next selected another two or more vectors at least 15 degrees away from the vector first selected. In other words, there were at least 10 vectors in between these vectors. Only the plaque portions, the thickness of which was more than 0.5 mm, were selected. The RF signals were excluded when the signals were from the regions with significant nonuniform rotational distortion, calcification, or drop-out in the conventional IVUS image. A total of 85 vectors were analyzed from all plaques imaged.

**Wavelet analysis.** We analyzed the IVUS RF signals offline by wavelet analysis (25) using MATLAB data processing software (The MathWorks, Natick, Massachusetts). Wavelet analysis is a signal-processing tool that enables the detection of a special geometric pattern within a localized area of a signal. A wavelet is a short segmental waveform of limited duration that has an average value of zero. Wavelet patterns that meet various mathematical

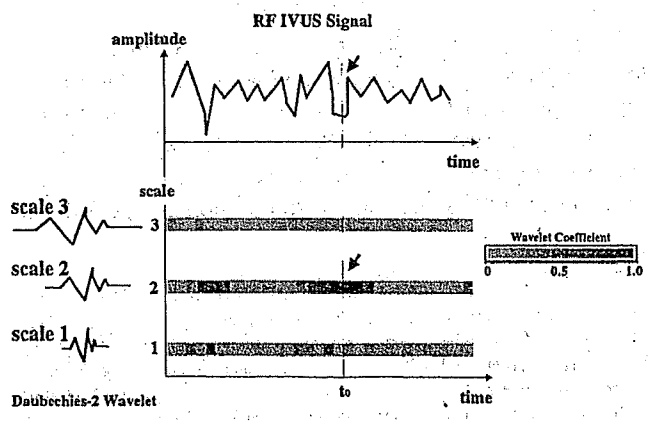


**Figure 2.** Procedure of wavelet analysis. In this example, a wavelet is stretched twice and three times. At a time of t0, a high value of wavelet coefficient is provided (arrow), suggesting that a special wave pattern similar to the wavelet of scale 2 is included within the signal at the time. IVUS = intravascular ultrasound; RF = radiofrequency.

JACC Vol. 45, No. 12, 2005
June 21, 2005:1954–60

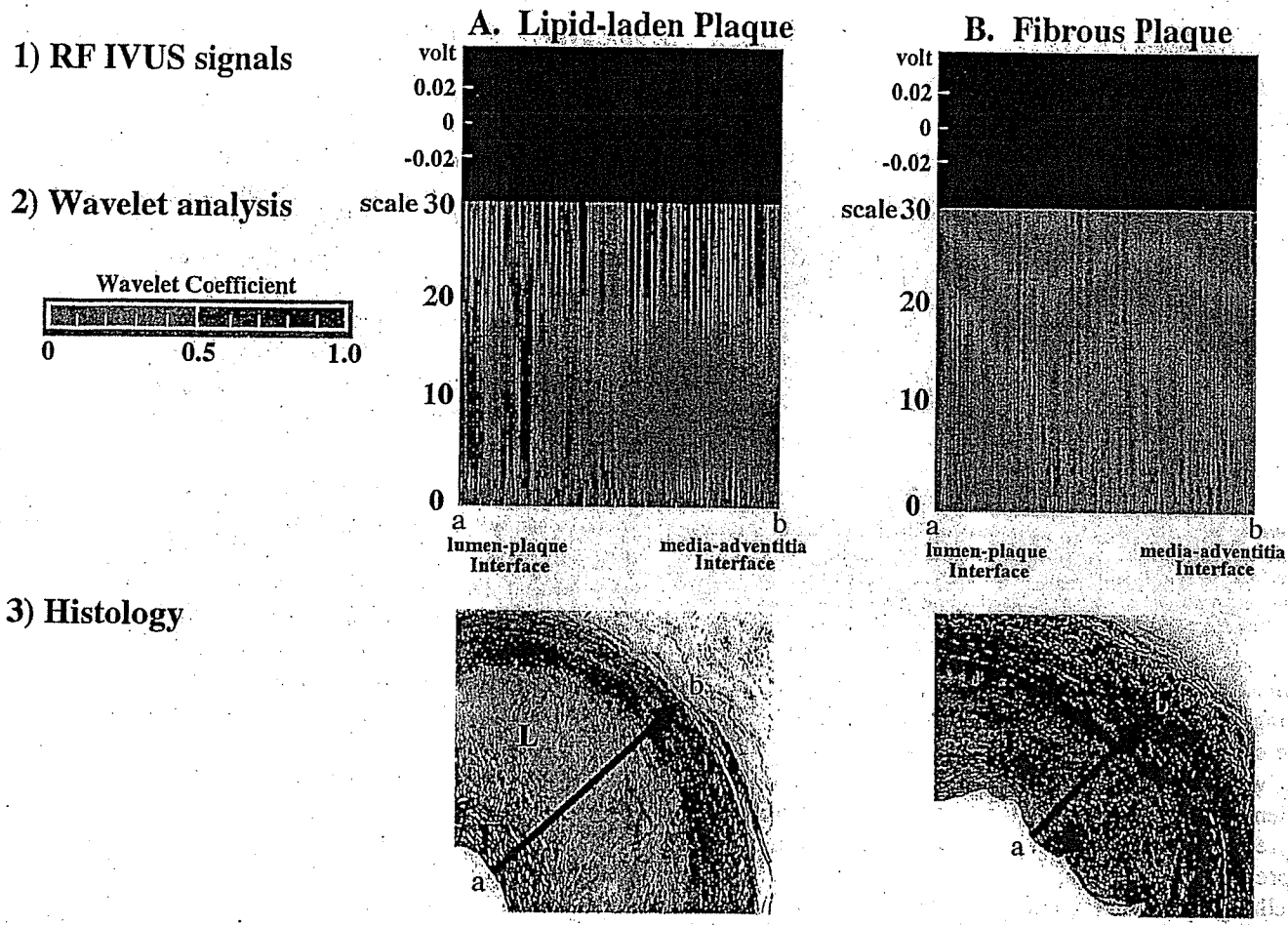


**Figure 3.** Representative examples of in vitro wavelet analysis of radiofrequency (RF) intravascular ultrasound (IVUS) signals from a lipid-laden plaque (**A**) and from a fibrous plaque without a lipid core (**B**). The **upper panels** show RF signals, the **middle panels** show the results of wavelet analysis, and the **lower panels** show the histologic specimen of the corresponding arterial cross section with Masson's trichrome. In the time-scale domain color-coded mapping of wavelet analysis, an apparently different pattern of pink area from an RF signal vector of a lipid-laden plaque is observed between scale 20 and scale 30, compared with the fibrous plaque. F = fibrous area; L = lipid core.

criteria have been proposed for comparison, such as Daubechies, Meye, and Mexican hat. Wavelet analysis involves the breaking up of a signal into shifted and scaled versions of the original (or mother) wavelet. The continuous wavelet transform is defined as the sum over time of the signal multiplied by scaled, shifted versions of the wavelet function:

$$C(scale, position) = \int_{-\infty}^{\infty} f(t)\psi(scale, position, t)dt$$

This results in many wavelet coefficients, $C$, which are a function of scale and position. Multiplying each coefficient by the appropriately scaled and shifted wavelet yields the constituent wavelets of the original signal. Wavelet analysis then produces a time-scale view of a signal. "Scaling a wavelet" means stretching (or compressing) it. The greater the scale factor, the more the wavelet is stretched. This scale is related to the frequency of the signal. "Shifting a wavelet" simply means delaying (or hastening) its onset.

To obtain a wavelet analysis, the following steps are performed (Fig. 2)

1. Take a wavelet and compare it to a section at the start of the original signal.
2. Calculate $C$, the coefficient between the section and the wavelet, which represents how closely correlated the wavelet is with this section of the signal. The higher $C$ is, the greater the similarity. The results will depend on the shape of the wavelet selected.
3. Shift the wavelet to the right and repeat steps 1 and 2 until the whole signal is covered.
4. Scale (stretch) the wavelet and repeat steps 1 through 3.
5. Repeat steps 1 through 4 for all scales.

This process produces wavelet coefficients ($C$) that are a function of scale and position. The commercially available program for wavelet analysis used in this study automatically selected the minimal scale of the wavelet to correspond to the minimum sampling interval.

After taking these steps, the coefficients are produced at different scales by different sections of the signal. The coefficients constitute a regression of the original signal performed on the wavelets. The results can be repre-

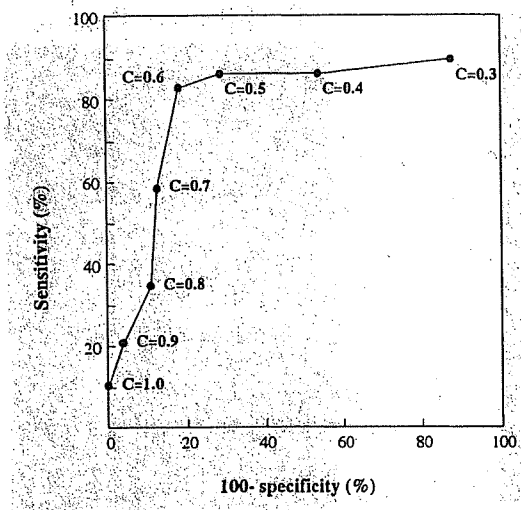


**Figure 4.** Receiver operating curve analysis was performed with varying degrees of the wavelet coefficient in terms of the capability of the in vitro detection of lipid-laden plaque. This analysis revealed that the optimal value of this wavelet coefficient to discriminate a lipid-laden plaque was 0.6. C = the wavelet coefficient.

sented graphically, in which the x-axis represents position along the signal (time), the y-axis represents scale, and the color at each x-y point represents the magnitude of the wavelet coefficient *C*. In this map, correlation coefficients are shown using a blue-pink scale, in which pink represents higher values of the coefficient and blue represents lower values.

**Preliminary in vivo application.** The same technique was applied in vivo to 29 coronary plaque segments from 13 patients (65 ± 6 years; range, 54 to 74 years) with coronary artery disease (7 patients with stable angina, 6 with acute coronary syndrome). The RF IVUS signals were obtained from the thickest part of the plaque imaged. These segments were excised by directional coronary atherectomy (FLEXI-CUT/Guidant, Indianapolis, Indiana) and processed for histologic analysis. Plaque segments were excluded, which were insufficiently debulked by the atherectomy, leaving a residual plaque area of more than one-third of the original plaque area. In the histologic preparation, the specimens were stained with hematoxylin-eosin stain and Azan stain. This study was approved by the institutional review committee, and patients gave informed consent.

**Histologic study.** In the in vitro study, after the arteries were imaged by IVUS, the needle for acoustic reference was removed, and the needle site marked with India ink. The specimens were processed for histology and stained with Masson's trichrome stain. The IVUS and the histologic examinations were performed by different observers. A plaque was defined as lipid-laden by visual inspection, when a lipid-core was >50% of the total plaque area. A lipid core was defined as a contiguous area of lipid-containing foam cells, extracellular lipids, cholesterol crystals, a lipid pool, or necrotizing material. A plaque was defined as fibrous when it had no distinct lipid core but had a fibroacellular matrix with dense collagen bands. The thickness of the lipid core had to be >0.3 mm and >50% of the total plaque area to be included in this study.

In the in vivo study, the directional coronary atherectomy specimens were stained with hematoxylin-eosin and Azan stains. This study only included typical fatty-dominant or fibrous-dominant plaques. The fatty-dominant plaques contained a lipid core >80% of total plaque area. The fibrous-dominant plaques contained a fibrous area >80% of total plaque area.

**Statistical analysis.** Values were expressed as means ± standard deviation. Receiver operating curve analysis was performed to discriminate the optimal criteria in the interpretation of the results of this wavelet analysis.

## RESULTS

**In vitro study.** The mean thickness of plaque examined in this study was 1.42 ± 0.47 mm. Histologic examination revealed that 29 of 85 vectors of RF signals analyzed were from a lipid-laden plaque. Representative examples of wavelet analysis of RF IVUS signals from a lipid-laden plaque and from a fibrous plaque are shown in Figure 3. Wavelet analysis of the RF signals with a Daubechies-2 wavelet function provided an apparently different pattern in the color-coded mapping between scale 20 and scale 30. In this time-scale graphic representation of wavelet analysis of RF IVUS signals from a plaque with a lipid core, a different pattern of pink mapping was observed that was not observed from a fibrous plaque without a lipid core. A lipid-laden zone frequently was present, when the wavelet coefficient (*C*) was more than a certain value compared with a wavelet whose scale is between 20 and 30. The ROC analysis revealed that the optimal value of this wavelet coefficient was 0.6 to discriminate a lipid-laden plaque (Fig. 4). Using this criteria, the lipid-laden plaque was detected in this in vitro setting with a sensitivity of 83% (24 of 29) and a specificity of 82% (46 of 56) (Table 1). Many other wavelet approaches (approximately 50 types) were analyzed, and none provided the sensitivity and specificity of the Daubechies-2 method.

**In vivo study.** Histologic examination from the directional coronary atherectomies revealed that 16 of 29 coronary segments were fat-dominant (lipid-laden). No apparent fatty area was observed histologically in the remaining 13 segments. In the lipid-laden plaques, the wavelet analysis with the Daubechies-2 wavelet function revealed a similar

**Table 1.** Sensitivity and Specificity of Wavelet Analysis of Radiofrequency Intravascular Ultrasound Signals for Detecting Lipid-Laden Plaque

| Histology | | Wavelet Coefficient ≥0.6 | Wavelet Coefficient <0.6 |
|---|---|---|---|
| Lipid core (+) | in vitro (n = 29) | 24/29 (83%) | 5/29 (17%) |
| | in vivo (n = 16) | 13/16 (81%) | 3/16 (19%) |
| Lipid core (−) | in vitro (n = 56) | 10/56 (18%) | 46/56 (82%) |
| | in vivo (n = 13) | 2/13 (15%) | 11/13 (85%) |

JACC Vol. 45, No. 12, 2005
June 21, 2005:1954–60

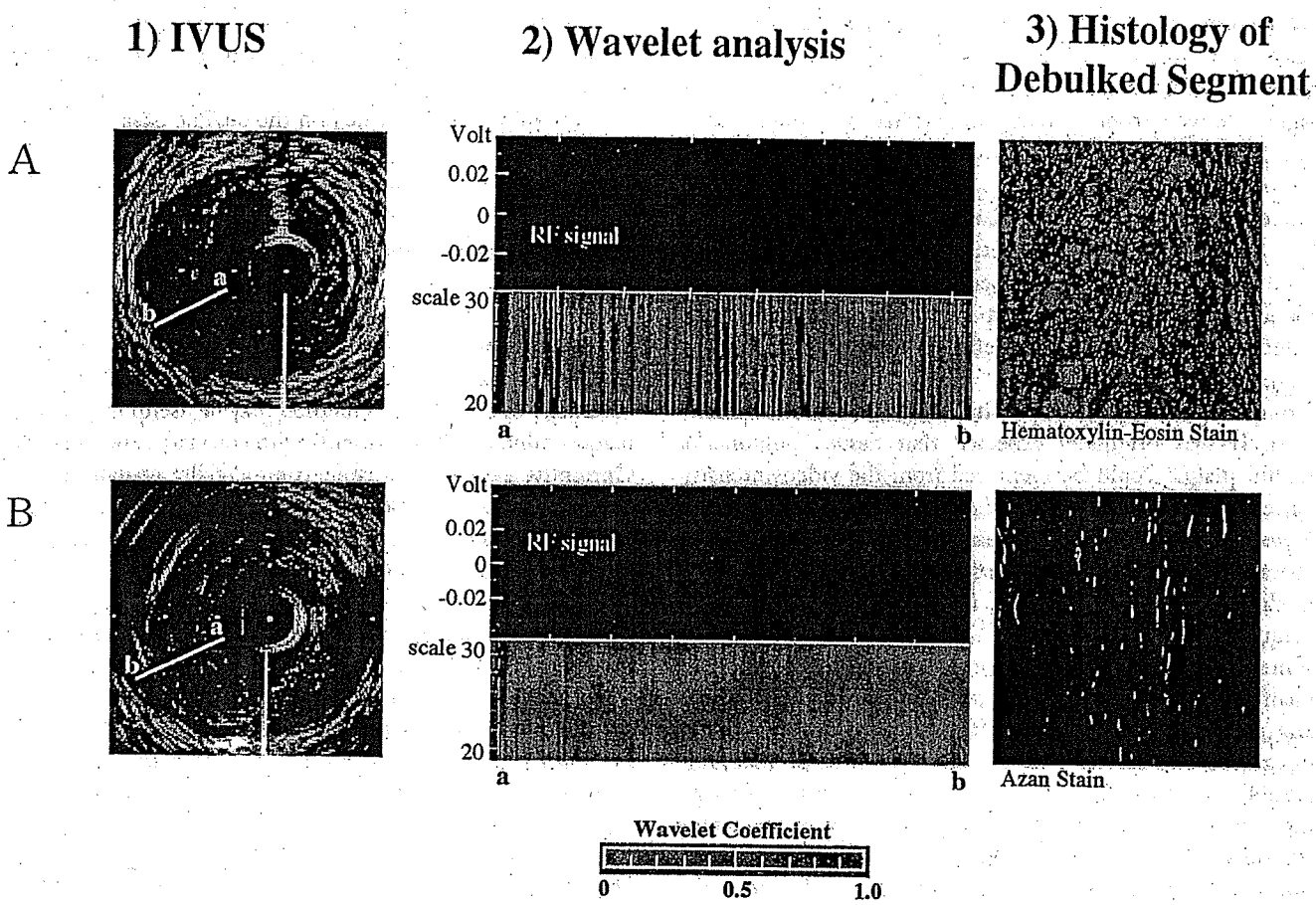


**Figure 5.** Representative examples of in vivo wavelet analysis of radiofrequency (RF) intravascular ultrasound (IVUS) signals from a lipid-laden plaque **(A)** and from a fibrous plaque without a lipid core **(B)**. The **left panels** show conventional IVUS images, the **middle panels** show the results of wavelet analysis, and the **right panels** show the histologic cross sections of the corresponding directional coronary atherectomy specimen with hematoxylin-eosin and Azan stains. A similar pattern of color mapping was observed from the radiofrequency signal vector of a lipid-laden plaque, as seen in the in vitro study.

pattern as the in vitro results (Fig. 5). Using the same criteria of the wavelet analysis as in the in vitro study, fatty plaque could be detected from the clinical material with a sensitivity of 81% (13 of 16) and a specificity of 85% (11 of 13).

## DISCUSSION

The present study is the first report of in vitro as well as in vivo tissue characterization of atherosclerotic plaque using a wavelet analysis of RF IVUS signals. The major finding of this study is that this wavelet method is accurate in detecting lipid-laden atherosclerotic plaque. This method may be useful in assessing plaque vulnerability in patients with coronary artery disease.

**Advantages of wavelet analysis.** The theoretical basis of wavelet analysis was first developed by Grossmann and Morlet in 1983 (25). Wavelet analysis is a time-frequency domain analysis of signals. The most well known of these is Fourier analysis, which breaks down a signal into constituent sinusoids of different frequencies. The Fourier transform was modified into a transform to analyze only a small section of the signal at a time by looking at "windows" of the signal. This short-time Fourier transform provides some information about when and at what frequencies a signal event occurs. The major drawback of this method is that once a particular size for the time window is chosen, that window is the same for all frequencies. If the window size is changed to a shorter one to increase time (space) resolution, the frequency resolution is compromised. Wavelet analysis was proposed in an attempt to overcome the problems in resolution.

Wavelet analysis represents a windowing technique with variable-sized regions. Wavelet analysis allows the use of long-time intervals when more precise low-frequency information is needed and shorter regions when high-frequency information is needed. One major advantage of wavelets is their ability to analyze a localized area of a larger signal. In this study, the Daubechies-2 wavelet proved best for detecting a lipid-laden plaque. An empirical selection of wavelet has to be made when applying wavelet analysis in a novel field of data. If a new wavelet family is developed, the sensitivity and specificity for detection of fatty tissue may be improved.

Wavelet scales 20 and 30 correspond to wavelengths of 32 and 47 $\mu$m, respectively. A scale of $<20$ is less than conventional IVUS resolution (26) or the ultrasound pulse

wavelength. The results from wavelet analysis with a wavelet scale <20 would measure artificial noise only. A higher value of wavelet correlation coefficient represents an acoustic signal derived from a more complicated structure. Compared with a fibrous area, a fatty area usually is composed of various kinds of tissue, such as lipid-laden foam cells, cholesterol crystals, extracellular lipids, necrotizing material, and fibers, which may be intermingled in a way that could produce complex acoustic impedance mismatches inside the plaque (17). Therefore, a lipid-laden area provides a higher value of wavelet correlation coefficient with a shorter scale of wavelet.

**Comparison with other methods of tissue characterization.** It was originally expected that tissue components within plaque could be identified from the video-intensity pattern of IVUS images (4,5,7,12–15). Subsequent studies, however, demonstrated significant limitations of tissue characterization by IVUS intensity patterns alone, especially in discriminating fibrous and fatty tissues or in assessing plaque vulnerability (16–19). To overcome the limitations, some authors (20–23) have proposed several methods of quantitative tissue characterization to discriminate fibrous and fatty plaque, including RF signal analysis, such as integrated backscatter analysis, attenuation slope mapping (19,24), and spectral analysis (27). Recently, IVUS elastography was proposed as a novel modality of tissue characterization with IVUS (28). Our laboratory previously reported that color mapping of the angle-dependent echo-intensity was useful for detecting fibrous caps within plaques (29). However, this method has difficulties in detecting other type of tissues. Because none of these previously reported techniques has become available commercially, no study has yet compared their clinical feasibility using the same subjects.

**Study limitations.** For the in vitro study, the arteries were imaged after they were fixed in formalin at room temperature. It is unknown whether formalin fixation or change in temperature will alter the results of this analysis. Another limitation was the use of nonpressure-distended arteries. When removed from physiologic pressure, atherosclerotic arteries contract. This contraction could significantly alter the architecture, which might affect the wave pattern of the RF IVUS signal. However, the in vivo application of the wavelet analysis also offered similar sensitivity and specificity for identifying a lipid-laden plaque as in the in vitro study. Therefore, these effects appear to be negligible in this study.

This wavelet analysis was performed for one single vector. The single vector analysis is subject to mismatch because of rotation of the images. To minimize any mismatch, we superimposed a radial line from the catheter center onto a conventional cross-sectional IVUS video image to enable the recognition of the location of each vector. In the in vitro study, all the plaques analyzed had a thickness >0.5 mm, and any lipid core had a thickness >0.3 mm. Therefore, we do not know whether it is possible to analyze thinner plaques or to identify very thin lipid cores with this method. Furthermore, the presence of blood and phasic pressure within the lumen as well as any noncoaxial alignment of the catheter may impair appropriate analysis in vivo with this method.

This study was performed on the off-line basis, taking an hour or so to obtain each color map. Therefore, a further development is necessary to be able to provide an on-line plaque evaluation during the study so that immediate feedback is given to the operator.

**Conclusions.** The present study demonstrates the feasibility of in vitro as well as in vivo tissue characterization by wavelet analysis of RF IVUS signals. Using wavelet analysis, lipid-laden plaque could be detected with a sensitivity and specificity of >80%. This method may be useful in assessing plaque vulnerability in patients with coronary artery disease. Currently, there is no reliable, commercially available device that is capable of discriminating fibrous and fatty areas within atherosclerotic plaque. Detection of vulnerable plaque or sequential observations of the stabilizing effect of lipid-lowering therapy on plaque composition with acceptable accuracy in vivo could improve the management of patients with coronary artery disease. Further evaluation of wavelet analysis in comparison with clinical data and inflammatory markers will be necessary to assess its usefulness in clinical practice to predict future cardiac events in patients with coronary artery disease.

**Reprint requests and correspondence:** Dr. Takafumi Hiro, Division of Cardiovascular Medicine, The Department of Medical Bioregulation, Yamaguchi University Graduate School of Medicine, 1-1-1 Minami Kogushi, Ube, Yamaguchi 755-8505, Japan. E-mail: thiro@yamaguchi-u.ac.jp.

## REFERENCES

1. Fuster V, Badimon L, Badimon J, et al. The pathogenesis of coronary artery disease and the acute coronary syndromes. N Engl J Med 1992;326:242–50, 310–8.
2. Libby P. The molecular basis of the acute coronary syndromes. Circulation 1995;91:2844–50.
3. Yock PG, Johnson EL, Linker DT. Intravascular ultrasound: development and clinical potential. Am J Card Imaging 1988;2:185–93.
4. Gussenhoven EJ, Essed CE, Lancee CT, et al. Arterial wall characteristics determined by intravascular ultrasound imaging: an in vitro study. J Am Coll Cardiol 1989;14:947–52.
5. Tobis JM, Mallery J, Mahon D, et al. Intravascular ultrasound imaging of human coronary arteries in vivo. Analysis of tissue characterizations with comparison to in vitro histological specimens. Circulation 1991; 83:913–26.
6. Mallery JA, Tobis JM, Griffith J, et al. Assessment of normal and atherosclerotic arterial wall thickness with an intravascular ultrasound imaging catheter. Am Heart J 1990;119:1392–400.
7. Nissen SE, Grines CL, Gurley JC, et al. Application of a new phased-array ultrasound imaging catheter in the assessment of vascular dimensions: in vivo comparison to cineangiography. Circulation 1990; 81:660–6.
8. Potkin BN, Bartorelli AL, Gessert JM, et al. Coronary artery imaging with intravascular high-frequency ultrasound. Circulation 1990;81: 1575–85.
9. Nissen SE, Gurley JC, Grines CL, et al. Intravascular ultrasound assessment of lumen size and wall morphology in normal subjects and patients with coronary artery disease. Circulation 1991;84:1087–99.
10. Nishimura RA, Edwards WD, Warnes CA, et al. Intravascular ultrasound imaging: in vitro validation and pathologic correlation. J Am Coll Cardiol 1990;16:145–54.

11. Hodgson JM, Graham SP, Savakus AD, et al. Clinical percutaneous imaging of coronary anatomy using an over-the-wire ultrasound catheter system. Int J Card Imaging 1989;4:187–93.
12. Di Mario C, The SH, Madretsma S, et al. Detection and characterization of vascular lesions by intravascular ultrasound: an in vitro study correlated with histology. J Am Soc Echocardiogr 1992;5:135–46.
13. Friedrich GJ, Moes NY, Muhlberger VA, et al. Detection of intralesional calcium by intracoronary ultrasound depends on the histologic pattern. Am Heart J 1994;128:435–41.
14. Bartorelli AL, Potkin BN, Almagor Y, et al. Plaque characterization of atherosclerotic coronary arteries by intravascular ultrasound. Echocardiography 1990;7:389–95.
15. Peters RJ, Kok WE, Havenith MG, et al. Histopathologic validation of intracoronary ultrasound imaging. J Am Soc Echocardiogr 1994;7: 230–41.
16. Hiro T, Leung CY, Russo RJ, et al. Variability in tissue characterization of atherosclerotic plaque by intravascular ultrasound: a comparison of four intravascular ultrasound systems. Am J Card Imaging 1996; 10:209–18.
17. Hiro T, Leung CY, De Guzman S, et al. Are soft echoes really soft? Intravascular ultrasound assessment of mechanical properties in human atherosclerotic tissue. Am Heart J 1997;133:1–7.
18. Kimura BJ, Bhargava V, DeMaria AN. Value and limitations of intravascular ultrasound imaging in characterizing coronary atherosclerotic plaque. Am Heart J 1995;130:386–96.
19. Jeremias A, Kolz ML, Ikonen TS, et al. Feasibility of in vivo intravascular ultrasound tissue characterization in the detection of early vascular transplant rejection. Circulation 1999;100:2127–30.
20. Bridal SL, Fornes P, Bruneval P, et al. Parametric (integrated backscatter and attenuation) images constructed using backscattered radio frequency signals (25–56 MHz) from human aortae in vitro. Ultrasound Med Biol 1997;23:215–29.
21. Linker DT, Yock PG, Gronningsaether A, et al. Analysis of backscattered ultrasound from normal and diseased arterial wall. Int J Card Imaging 1989;4:177–85.
22. Kawasaki M, Takatsu H, Noda T, et al. Non-invasive tissue characterization of human atherosclerotic lesions in carotid and femoral arteries by ultrasound integrated backscatter: comparison between histology and integrated backscatter images before and after death. J Am Coll Cardiol 2001;38:486–92.
23. Kawasaki M, Takatsu H, Noda T, et al. In vivo quantitative tissue characterization of human coronary arterial plaques by use of integrated backscatter intravascular ultrasound and comparison with angioscopic findings. Circulation 2002;105:2487–92.
24. Wilson LS, Neale ML, Talhami HE, et al. Preliminary results from attenuation-slope mapping of plaque using intravascular ultrasound. Ultrasound Med Biol 1994;20:529–42.
25. Daubechies I, Grossmann A. An integral transform related to quantization. J Mat Phys 1980;21:2080–90.
26. Benkeser PJ, Churchwell AL, Lee C, et al. Resolution limitations in intravascular ultrasound imaging. J Am Soc Echocardiogr 1993;6: 158–65.
27. Nair A, Kuban BD, Tuzcu EM, et al. Coronary plaque classification with intravascular ultrasound radiofrequency data analysis. Circulation 2002;106:2200–6.
28. de Korte CL, Sierevogel MJ, Mastik F, et al. Identification of atherosclerotic plaque components with intravascular ultrasound elastography in vivo: a Yucatan pig study. Circulation 2002;105: 1627–30.
29. Hiro T, Fujii T, Yasumoto K, et al. Detection of fibrous cap in atherosclerotic plaque by intravascular ultrasound by use of color mapping of angle-dependent echo-intensity variation. Circulation 2001;103:1206–11.

Journal of the American College of Cardiology
© 2005 by the American College of Cardiology Foundation
Published by Elsevier Inc.

Vol. 46, No. 8, 2005
ISSN 0735-1097/05/$30.00
doi:10.1016/j.jacc.2005.06.069

# Longitudinal Structural Determinants of Atherosclerotic Plaque Vulnerability

## A Computational Analysis of Stress Distribution Using Vessel Models and Three-Dimensional Intravascular Ultrasound Imaging

Koji Imoto, MD,* Takafumi Hiro, MD, PHD,* Takashi Fujii, MD, PHD,* Akihiro Murashige, MD, PHD,* Yusaku Fukumoto, MD,* Genta Hashimoto, MD,* Takayuki Okamura, MD, PHD,* Jutaro Yamada, MD, PHD,* Koji Mori, PHD,† Masunori Matsuzaki, MD, PHD, FACC*

*Ube, Japan*

**OBJECTIVES** This study theoretically examined the longitudinal structural determinants of plaque vulnerability using a color-coded stress mapping technique for several hypothetical vessel models as well as three-dimensional intravascular ultrasound (IVUS) images with use of a finite element analysis.

**BACKGROUND** It has been shown that an excessive concentration of stress is related to atherosclerotic plaque rupture. However, the local determinants of in-plaque longitudinal stress distribution along the coronary arterial wall remain unclear.

**METHODS** Using a finite element analysis, we performed a color mapping of equivalent stress distribution within plaques for three-dimensional vessel models as well as longitudinal IVUS plaque images (n = 15). Then, the effects of plaque size, shape, expansive remodeling, calcification, and lipid core on the equivalent stress distribution were examined.

**RESULTS** The color mapping of vessel models revealed a concentration of equivalent stress at the top of the hills and the shoulders of homogeneous fibrous plaques. Expansive remodeling and the lipid core augmented the surface equivalent stress, whereas luminal stenosis and superficial calcification attenuated the equivalent stress. The location of excessive stress concentration was modified by the distribution of the lipid core and calcification. The thickness of the fibrous cap was inversely related to the equivalent stress within the fibrous cap. However, the color mapping of IVUS plaque images showed that the equivalent stress value at the fibrous cap varied with changes in plaque shape and superficial calcification, even when the thickness of the fibrous cap remained constant.

**CONCLUSIONS** A distribution analysis of longitudinal stress revealed specific effects of plaque shape, size, and remodeling, as well as effects of the interior distribution of tissue components, on the concentration of stress at the plaque surface. Moreover, fibrous caps of the same thickness did not consistently represent the same vulnerability to rupture. (J Am Coll Cardiol 2005;46: 1507–15) © 2005 by the American College of Cardiology Foundation

Plaque rupture is a major cause of acute coronary syndrome (1,2). It has been shown that plaque rupture frequently occurs in a noncalcified eccentric atherosclerotic plaque with nonsevere stenosis (3–8), expansive remodeling (9–12), a thin fibrous cap (4,13–17), a large lipid core (4,13–16,18–21), and macrophage infiltration (17,22). Therefore, it is thought that a particular cluster of plaque, referred to as vulnerable plaques, is likely to exist, and the development of a modality for detecting this potentially vulnerable portion in the coronary arterial wall is greatly needed in the clinical setting.

In the process of plaque rupture, an excessive concentration of stress at a certain portion of the plaque surface is considered an important factor (23). An in vitro study reported by Loree et al. (13) showed that thinning of the fibrous cap over a subintimal lipid pool dramatically increased peak circumferential stress in the cross section, especially at the shoulder region of eccentric plaques. However, the local determinants of the distribution of in-plaque longitudinal stress along the coronary arterial wall remain unclear. Therefore, the purpose of this study was to clarify the determinants of the distribution of longitudinal stress within plaques, using a color mapping technique based on computational structural analysis. This color mapping was derived from several hypothetical vessel models as well as from three-dimensional intravascular ultrasound (IVUS) images. The structural computation was performed by a finite element analysis using established material parameters for vessel tissue components (13,19,23,24).

From the Departments of *Molecular Cardiovascular Biology and †Applied Medical Engineering Science, Yamaguchi University Graduate School of Medicine, Yamaguchi, Ube, Japan. This study was partly supported by a grant-in-aid for scientific research of the Ministry of Education, Japan (grant No. (C)(2)14570666), Health and Labour Sciences Research Grants: Comprehensive Research on Cardiovascular Diseases from Ministry of Health, Labour, and Welfare of Japan, and Knowledge Cluster Initiative of the Ministry of Education, Japan. The first two authors contributed equally to this work. This study was presented in part at the 77th scientific sessions of the American Heart Association, New Orleans, Louisiana, 2004.

Manuscript received February 6, 2005; revised manuscript received June 10, 2005, accepted June 14, 2005.

## METHODS

**Design of vessel models.** Initially, various idealized vessel models were designed to examine the effects of plaque morphology and tissue components on longitudinal stress

JACC Vol. 46, No. 8, 2005
October 18, 2005:1507–15

Abbreviations and Acronyms
E = Young moduli
G = shear modulus
IVUS = intravascular ultrasound
P = Poisson ratios

distribution inside the plaque. As shown in Figure 1, a cylindrical vessel model was used, in which an atherosclerotic plaque was formed by the revolution of the same longitudinal sectional structure, thereby avoiding the influence of cross-sectional geometrical factors. This cylindrical model had an inner radius of 1.7 mm and a vessel wall thickness of 0.5 mm at the reference site. In the computational simulation, various plaque morphologies were hypothesized with various stenosis severities and types of vessel remodeling. It was assumed that the plaque components consisted of collagen fibers, calcifications, homogenous lipid tissue, and smooth muscle cells. The blood pressure was considered to be uniform along the vessel walls. The effect of blood flow was neglected in this study. There were no structural limitations in terms of the degree of outward expansion.

As in previous established studies (13,23), all of the components of the atherosclerotic plaques were considered to be orthotropic materials with linear elastic properties. In this study, arteries and fibers provided similar material properties in the circumferential ($\theta$) direction, as well as in the axial (z) direction, which differed from those in the radial (r) direction. Each parameter for the material properties defined in this study is shown in Table 1. In Table 1, $E_r$ and $E_\theta$ are the Young moduli in the radial and circumferential directions, respectively. $G_{r\theta}$ is the shear modulus in the $r\theta$ plane, where $G_{ij}$ is the ratio of the shear stress to the shear strain in the $ij$ plane. $P_{r\theta}$ and $P_{\theta z}$ are the Poisson ratios in the $r\theta$ and $\theta z$ planes, respectively. All of these values have been accepted as the representative values of the material properties of atherosclerotic lesions (13,23). It was assumed that lipids and calcifications were nearly incompressible because of their isotropic properties (23). The Young modulus of lipids was estimated to be 1/100th of the circumferential modulus of a normal artery. The Young modulus of calcified plaques was estimated as 10 times that of the plaque $E_\theta$ (13).

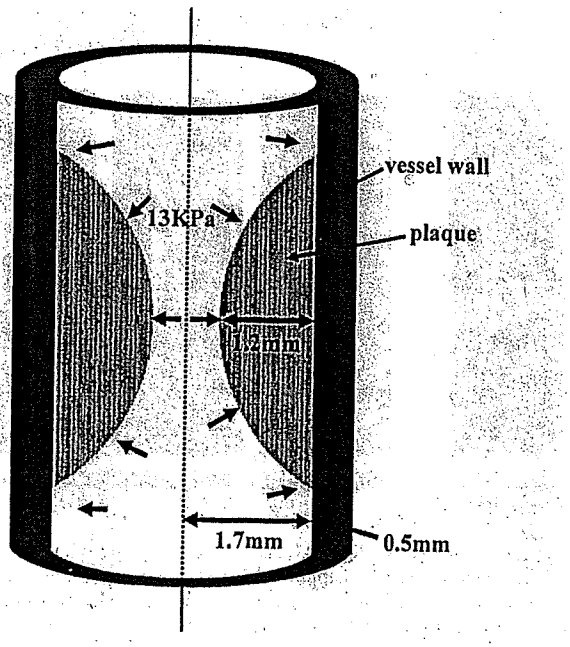


**Figure 1.** Three-dimensional model. In this vessel model, vessel diameter may vary when a remodeling model is considered.

**Structural analysis.** The computational structural analysis was performed with a finite element model using a commercially available application (ANSYS 6.0 software, ANSYS Inc., Pittsburgh, Pennsylvania). A complex structure of a vessel model was first divided into smaller subunits designated as elements. The total number of the subunits was approximately 10,000, with a spatial resolution of approximately 100 (10 $\mu$m × 10 $\mu$m) $\mu m^2$. Then, the equivalent stress for each element was calculated. The equivalent stress represented all types of stress for a certain area analyzed, which was calculated from three principal stresses. The structure was automatically meshed with eight-noded quadrilateral plane-strain elements. Each mesh was modified by using an adaptive remeshing algorithm, which was installed in the program. An internal luminal static pressure of 13 kPa (100 mm Hg) was applied along the luminal wall, representing the mean physiological blood pressure in the coronary arteries. Finally, contour plots of equivalent stress were shown on a post-graphics terminal. These contour plots provided two types of colorized mapping, with color codes superimposed on the original structure. One type of mapping was absolute mapping, in which each color code represented a certain range of the absolute value of the equivalent stress; the other type of mapping was relative mapping, in which the color coding was performed by equal division of the range of stress between the maximum and minimum values. According to the computer algorithm, the resulted deformation, such as indentation at the soft part or outward bulging of the normal wall without plaques, was also illustrated.

This study first analyzed the longitudinal stress distribution within plaques for several vessel models with varying structural characteristics of plaque, such as plaque size, plaque shape, stenosis severity, remodeling type, lipid core size, fibrous cap thickness, location and degree of calcification, and so on.

**IVUS study.** The present study also examined the longitudinal stress distribution in plaques, the structure of which was obtained from the three-dimensional IVUS images. Fifteen human ruptured coronary lesions selected from patients diagnosed with acute coronary syndrome were imaged by IVUS (Atlantis SR pro, 2.8-F, 40-MHz, Boston Scientific Corp./SCIMED, Maple Grove, Minnesota). The transducer was withdrawn automatically using a motorized pullback device (pullback speed, 0.5 mm/s). The IVUS images were all recorded on S-VHS videotape for off-line

**Table 1.** Material Parameters for Arteries, Plaques, Calcifications, and Lipids Used in Finite Element Models

| | Young Moduli (E) | | | Poisson Ratios (P) | | | Shear Moduli (G) | | |
|---|---|---|---|---|---|---|---|---|---|
| | r | θ | z | rθ | θz | zr | rθ | θz | zr |
| Artery | 10 | 100 | 10 | 0.01 | 0.27 | 0.27 | 50 | 50 | 50 |
| Plaque | 50 | 1000 | 50 | 0.01 | 0.27 | 0.27 | 500 | 500 | 500 |
| Calcification | 10,000 | 10,000 | 10,000 | 0.48 | 0.48 | 0.48 | | | |
| Lipid | 1 | 1 | 1 | 0.48 | 0.48 | 0.48 | | | |

r, θ, and z = radial, circumferential, and axial directions, respectively.

analysis. The images were then digitized and analyzed with commercially available software for longitudinal reconstructive IVUS image analysis (Netra IVUS, ScImage Inc., Los Altos, California).

The rupture was defined by an apparent morphology in IVUS images along with comparable clinical history, electrocardiograms, and echocardiograms. No definitive thrombus was detected around the plaque both in IVUS and in angiography. Ruptured plaques with a distinct cavity as well as a significant residual fibrous flap were selected to predict surface morphology before rupture by extrapolating the line of lumen-intima interface.

It was assumed that the ulceration cavity detected by IVUS used to be a lipid core, and that a fibrous cap of a certain thickness used to cover the lipid core. In this in vivo analysis, it was also presumed that the arteries and the plaque components had orthotropic linearly elastic material properties, and that the plaques consisted of homogeneous

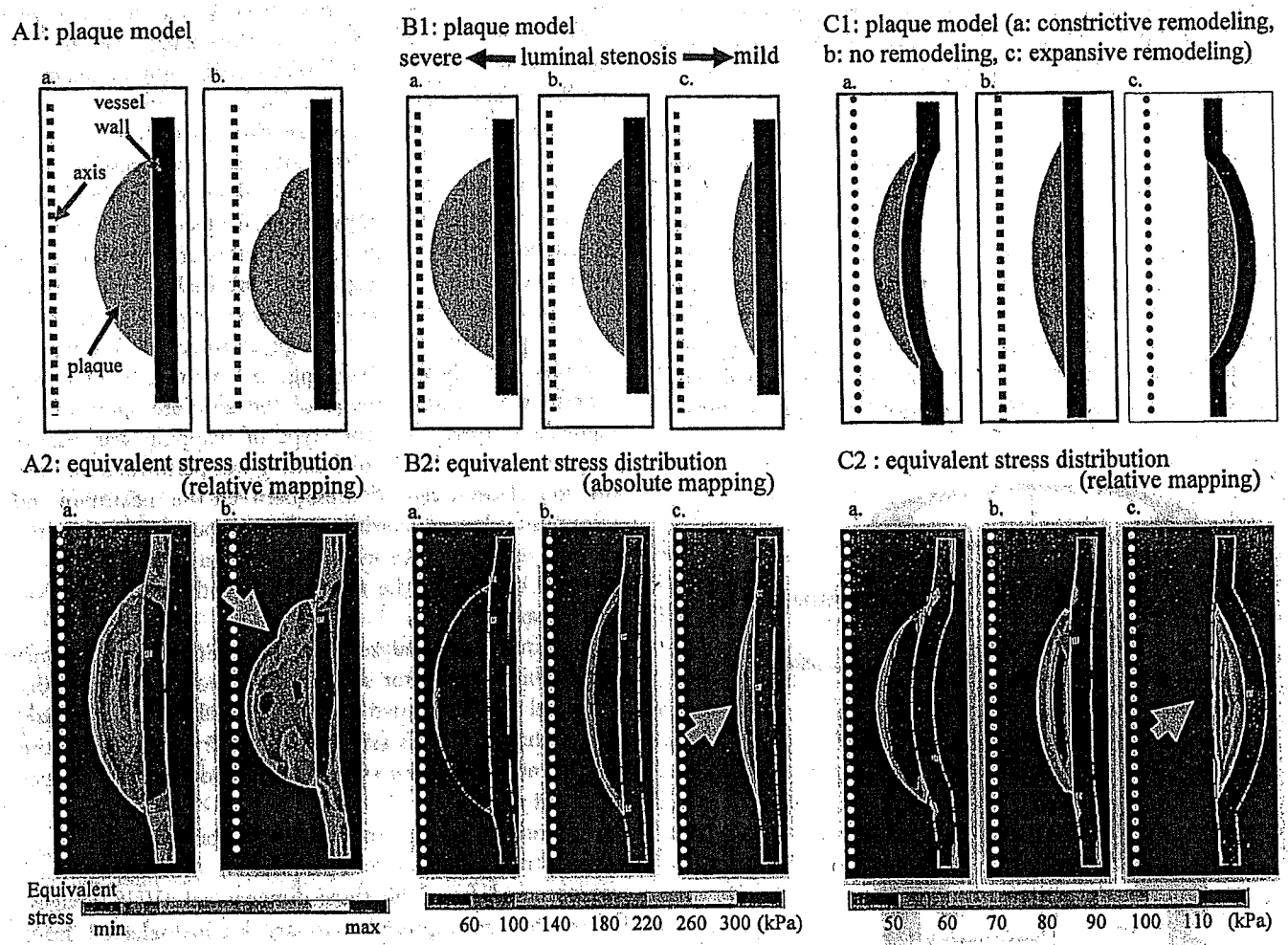


**Figure 2.** Relationship between stress distribution and plaque shape, luminal stenosis, or vessel remodeling. (A1, A2) Color mapping of longitudinal stress distribution within a homogeneous hill-like fibrous plaque model and a complex-shaped model. Relative mapping (A2) was performed in the automatically determined window between the maximum and minimum value of stress. The arrows designate the sites of stress concentration. (B1, B2) Relationship between luminal stenosis and stress distribution. Absolute mapping (B2) represents the distribution of the absolute value of equivalent stress. There was a negative relationship between the equivalent stress and luminal stenosis. (C1, C2) Relationship between vessel remodeling and stress distribution. The equivalent stress at the plaque surface of arteries with expansive remodeling was greater than that of arteries with constrictive remodeling, when the plaque thickness remained constant.